


 Cite this: *RSC Adv.*, 2020, 10, 15665

Structure and glass transition of amorphous materials composed of titanium-oxo oligomers chemically modified with benzoylacetone

 Shinya Oda,^a Shinji Kohara,^b  Ryo Tsutsui,^a Mamoru Kasasaku^a and Hiromitsu Kozuka^b *^c

Titanium-*n*-butoxide was hydrolyzed in the presence of benzoylacetone, and the resulting solution was concentrated and dried at 120 or 140 °C to obtain transparent amorphous materials. High-energy X-ray diffraction measurement was conducted at the SPring-8 facility, and the reduced pair distribution function, $G(r)$ was calculated by Fourier transform of the total structure factor, $S(Q)$. The $G(r)$ value suggested that the materials are composed of TiO_6 octahedra linked by corner- and edge-sharing. Low temperature thermomechanical analysis (TMA) and differential scanning calorimetry (DSC) were conducted on the materials, where a deflection was detected both in the TMA and DSC curves, revealing the glass transition of the materials. Combined with the previous work based on infrared absorption spectroscopy and gel permeation chromatography, the materials are demonstrated to be a new class of glassy materials composed of linked metal-oxygen polyhedra chelated with organic molecules. The materials are innovative due to the high refractive indices that originate in the metal-oxo oligomers and to the shapability given by their thermoplastic properties.

 Received 4th February 2020
 Accepted 13th April 2020

DOI: 10.1039/d0ra01047b

rsc.li/rsc-advances

Introduction

Metal-oxo clusters or polyoxometalate clusters are chemical species that are composed of metal-oxygen polyhedra linked together by shared oxygen atoms. They are attracting much attention because of their unique functions and availability as building blocks of new classes of organic-inorganic hybrid materials.¹⁻³ Related papers are significantly growing in number, and the active trends are well documented in excellent reviews by Long *et al.*,⁴ Proust *et al.*,⁵ and Kortz *et al.*⁶ There are two large streams in the studies. One is the synthesis of crystalline metal-oxo clusters and their structural analysis based on single crystal X-ray diffraction.⁷ The other is the application of clusters as building blocks of organic-inorganic hybrid materials utilizing their active functions.¹⁻³

Recently we have demonstrated that the hydrolysis of metal alkoxides in the presence of specific β -diketones, followed by concentration and drying, produces optically transparent materials that exhibit thermoplasticity. The specific β -diketones include 1-phenylbutane-1,3-dione (benzoylacetone, bzac), 1-

(morpholin-4-yl)butane-1,3-dione and 1,3-diphenylpropane-1,3-dione.⁸⁻¹⁰ Acetylacetone (acac), a different type of β -diketone, has often been used in the field of sol-gel technology to control the rate of hydrolysis of transition metal alkoxides.^{11,12} However, the gels prepared from acac-containing alkoxide solutions do not show such thermoplasticity, and are just hardened when heated, which results from the loss of acac followed by condensation reaction to allow metal-oxo bridges to be developed. In other words, thermoplastic properties have never been expected before our discovery of such gels derived from β -diketone-containing alkoxide solutions.

We have made some characterizations on the transparent, thermoplastic products obtained from titanium alkoxide solutions containing benzoylacetone (bzac) in previous works.^{9,10} X-ray diffraction (XRD) measurements showed that the products are amorphous.⁹ Infrared (IR) absorption spectroscopy evidenced the chelation of the titanium atoms by bzac.^{9,10} We also studied the molecular weight of the constituent species by gel permeation chromatography (GPC), finding that the polystyrene-based weight average molecular weight ranging from 150 to 630 increases with increasing water content and with decreasing bzac content in the starting solutions.¹⁰ It was also found that the materials composed of larger molecular weight oligomers exhibit higher softening temperatures in thermomechanical analysis (TMA) curves.^{9,10} These results strongly suggest that the materials are composed of titanium-oxo oligomers that are formed *via* hydrolysis and condensation of titanium alkoxides modified with bzac. The surface of

^aGraduate School of Science and Engineering, Kansai University, Suita, Osaka 564-8680, Japan

^bSynchrotron X-ray Group, Light/Quantum Beam Field Research Center for Advanced Measurement and Characterization, NIMS, 1-1-1 Kouto, Sayo-cho, Sayo-gun, Hyogo 679-5148, Japan

^cFaculty of Chemistry and Materials Engineering, Kansai University, Suita, Osaka 564-8680, Japan. E-mail: kozuka@kansai-u.ac.jp



the titanium-oxo oligomers may be covered with the hydrophobic segment of bzac, which leads to weak interaction between the oligomers, allowing thermoplasticity.

In spite of the results and discussions mentioned above, we still do not have direct experimental evidences that guarantee the titanium-oxo oligomers as the constituents of the materials. We do not know their structure either, *i.e.* the coordination number of the titanium atoms and the type of the linkage of the coordination polyhedra. Then the first purpose of the work is to clarify the structure of the constituents of the thermoplastic materials that are prepared from bzac-containing titanium alkoxide solutions. The structure was studied by high energy X-ray diffraction (HEXRD) measurement at SPring-8 and pair distribution function analyses.

The thermoplastic properties allow us to expect that such materials prepared from β -diketone-containing alkoxide solutions could be a new class of glass materials. Glasses are well known in oxides,¹³ chalcogenides,¹⁴ halides,¹⁵ metallic alloys,¹⁶ organic polymers,¹⁷ and organic molecules (the so-called "molecular liquids").¹⁸ Glassy states have also been reported recently in metal-organic-frameworks (MOF's).^{19,20} However, glassy states have never been reported in materials composed of metal-oxo oligomers modified with organic ligands. If glass transition is detected, such oxo oligomer-based materials will be recognized as a new class of glasses, which is scientifically interesting and important. The properties based on metal-oxygen polyhedra in conjunction with transparency and thermoplastic properties would also make them attractive from the viewpoint of engineering as novel functional materials that can be shaped near at room temperatures *via* injection molding or melt casting. For these reasons, the glass transition was examined for the materials prepared from bzac-containing titanium alkoxide solutions.

Experimental

Titanium-*n*-butoxide ($\text{Ti}(\text{OC}_4\text{H}_9)_4$), bzac and acetone (CH_3COCH_3) were purchased from Wako Pure Chemical Industries, Osaka, Japan. Bzac was dissolved in acetone, and then $\text{Ti}(\text{OC}_4\text{H}_9)_4$ and H_2O were added successively under magnetic stirring to prepare a starting solution of mole ratios, $\text{Ti}(\text{OC}_4\text{H}_9)_4 : \text{bzac} : \text{H}_2\text{O} : \text{CH}_3\text{COCH}_3 = 1 : 2 : 1 : 20$. The solution was concentrated at 80 °C for 50 min after stirring at room temperature for 1 h. A drop of the concentrated solution was placed on a sodalime silicate glass plate at 140 °C in nitrogen, kept there for 30 min to obtain a transparent solidified sample. Some of the samples thus obtained were heated successively in air at 200 and 250 °C for 10 min. These samples were served for HEXRD measurements.

For the samples for low-temperature TMA and low temperature differential scanning calorimetry (DSC), the concentrated solution was solidified by drying on a sodalime silicate glass plate at 120 °C for 40 min in air. The solidified product was heated again at 120 °C, where the product exhibited fluidity, and was put into a syringe. The sample in the syringe was poured at 120 °C in an aluminum cell 4.5 mm in diameter and 1 mm in depth and in that 5 mm in diameter and 5 mm in depth

for TMA and DSC measurements, respectively, and solidified again by cooling down to room temperature. The total time for heating at 120 °C was 120 min including the drying of the concentrated solution. Low temperature TMA was performed using a thermomechanical analyzer (TMA8310, Rigaku, Tokyo, Japan), where the sample was heated from -50 °C at a rate of 5 °C min^{-1} in flowing N_2 gas under a load of 98 mN. Low temperature DSC was conducted using a differential scanning calorimeter (DSC220, Seiko Instruments, Chiba), where the sample in the aluminum cell was sealed with an aluminum lid and heated from -50 °C at a rate of 5 °C min^{-1} .

The HEXRD measurements were carried out at the beamline BL04B2 of SPring-8 facility, Japan. The samples were crushed and placed in a silica glass tube of 2 mm in inner diameter and served for the measurements where an empty silica glass tube was used as the blank. The monochromatic X-rays of 61.4 keV were obtained using a Si(220) monochromator, and the measurement was conducted over the scattering vector, Q , of 0.2–21.0 \AA^{-1} . The observed diffraction profile was corrected for polarization, absorption, air scattering, and Compton scattering, and was normalized to give a structure factor, $S(Q)$. The reduced pair distribution function, $G(r)$, was calculated by Fourier transform of the $S(Q)$. The details of data analysis as well as the data analysis code are described in ref. 21.

Results and discussion

Fig. 1 shows the photograph of the solidified product that was prepared by dropping the concentrated solution on a square Si(100) substrate, followed by drying at 120 °C. The product was yellow and transparent, softening when heated. The product is amorphous as was demonstrated previously by XRD measurements.⁹ The configuration of the Ti–O polyhedra and their linkages in the solidified product are discussed below, based on their reduced pair distribution functions, $G(r)$. Fig. 2 shows the structure factors, $S(Q)$, of the solidified samples heated at 140, 200 and 250 °C where Fig. 2b is those enlarged in the vertical axis. It is seen that $S(Q)$ is similar between the samples heated at 140 and 200 °C but is different from that heated at 250 °C, where the sample heated at 250 °C has a much larger peak at the lowest Q (Fig. 2a). The chelating bzac is lost by thermal decomposition when the sample is heated up to 250 °C as was



Fig. 1 Photograph of the solidified product that was prepared by dropping the concentrated solution on a square Si(100) substrate, followed by drying at 120 °C.



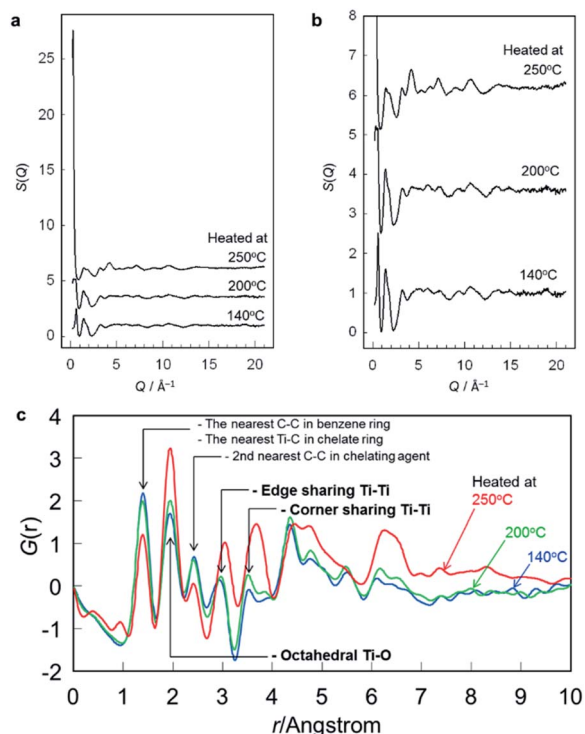


Fig. 2 (a) Structure factors, $S(Q)$, of the solidified samples heated at 140, 200 and 250 °C, and (b) those enlarged in the vertical axis. Successive curves are displaced upward for ease of viewing. (c) Reduced pair distribution functions, $G(r)$, of the solidified samples heated at 140, 200 and 250 °C, obtained from $S(Q)$.

previously demonstrated by infrared absorption spectroscopy.⁹ The much larger peak at the lowest Q in the sample heated at 250 °C may result from the formation of nanopores due to the loss of bzac. It was also revealed in the XRD patterns in the previous work,⁹ where a sharper diffraction peak was detected at small angles in the sample heated at 250 °C. The reduced pair distribution functions, $G(r)$, obtained from the $S(Q)$ is shown in Fig. 2c. The $G(r)$ peaks at 1.40 and 2.43 Å decreased when the sample was heated up to 250 °C, corresponding to the difference in $S(Q)$. Such a decrease indicates that the $G(r)$ peaks at 1.40 and 2.43 Å are related to chelating bzac, which are assigned to the first and second nearest C–C bond lengths in the benzene ring²² of bzac. Then these peaks will hereafter be neglected in discussion.

The first nearest Ti–O distances reported in literature for titanium–oxygen coordination polyhedra are summarized in

Table 1 First nearest Ti–O distance in titanium–oxygen coordination polyhedra^{23–26}

Coordination number	Ti–O distance (1st nearest neighbor)/Å
4	1.63–1.82
5	1.68, 1.96
6	1.70, 1.94–1.95
7	1.91–2.00

Table 2 Atomic distance in anatase and rutile crystals

Crystals	Atomic distance/Å		
	Ti–Ti	Ti–O	O–O
Anatase			
1st nearest neighbor	3.04	1.93, 1.98	2.47, 2.79, 3.04
2nd nearest neighbor	3.78	3.86	3.70, 3.78
3rd nearest neighbor	4.85	4.25, 4.27	3.96
4th nearest neighbor	5.35, 5.46	4.75	4.52
Rutile			
1st nearest neighbor	2.96	1.95, 1.98	2.54, 2.78, 2.96
2nd nearest neighbor	3.57	3.49, 3.56	3.32
3rd nearest neighbor	4.59	4.08	3.90, 3.96
4th nearest neighbor	5.46, 5.50	4.52, 4.57, 4.62	4.45, 4.59

Table 1. Prasai *et al.* reported that TiO_6 octahedra have Ti–O distances of 1.91–2.00 Å in rutile, anatase and amorphous titania.²³ On the other hand, Kaur *et al.* reported that TiO_4 tetrahedra in amorphous titania nanoparticles have Ti–O distances of 1.63–1.82 Å.²⁴ Cormier *et al.* reported that TiO_5 square pyramids in $\text{K}_2\text{O–TiO}_2\text{–SiO}_2$ glasses have four and one Ti–O distances of 1.96 and 1.68 Å, respectively.²⁵ Farges *et al.* also studied the Ti–O distances in the TiO_5 square pyramids in $(\text{Na}_2\text{O}, \text{K}_2\text{O})\text{–TiO}_2\text{–SiO}_2$ glasses, reporting the distances of the four and one Ti–O bonds to be 1.94–1.95 and 1.70 Å, respectively.²⁶ Then the peak detected at 1.94 Å in Fig. 2c is assigned to the first nearest Ti–O distance, and most of the titanium species may be present as TiO_6 octahedra in the solidified product.

Table 2 summarizes the Ti–Ti, Ti–O and O–O distance in anatase and rutile calculated using VESTA program.²⁷ It is seen that rutile has the second nearest Ti–Ti distances of 2.96 and 3.57 Å while anatase has those of 3.04 and 3.78 Å. The shorter and longer distances correspond to those in edge- and corner-shared octahedra, respectively. Then it is reasonable to assign the $G(r)$ peaks at 2.94 and 3.53 Å to the Ti–Ti distances in edge- and corner-shared TiO_6 octahedra, respectively. Other atomic pair peaks possibly overlap with those of such Ti–Ti pairs. Rutile has an O–O distance of 2.96 Å and Ti–O distances of 3.49 and 3.56 Å (Table 2), which can overlap with the Ti–Ti distances. The nearest Ti–C distance in a titanium complex with chelating bzac is *ca.* 3.0 Å,²⁸ which can also overlap with the Ti–Ti distance of

Table 3 Atomic distance in a chelating ring of Ti–BzAc²⁷

Atomic pair	Atomic distance (1st nearest neighbor)/Å
Ti–O	1.98–2.08
Ti–C	3.00–3.05
O–C	1.27–1.31



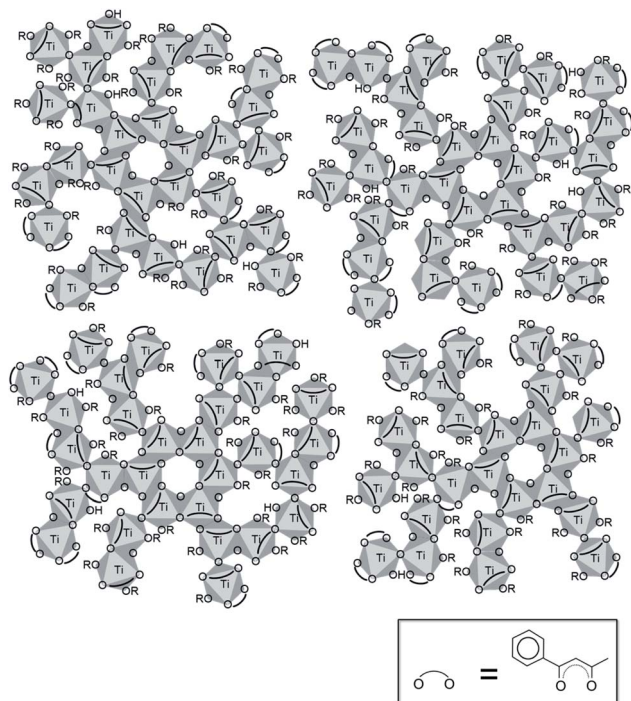


Fig. 3 Structure model for the solidified product prepared from the titanium-*n*-butoxide solution containing bzac.

2.94 Å (Table 3). The Ti-Ti peak at 3.53 Å has a shoulder at 3.81 Å. Kaur *et al.* reported that the second nearest Ti-O distance is 3.78 Å in amorphous titania nanoparticles composed of *ca.* 55% TiO₆, 32% TiO₅, 7% TiO₄ and 5% TiO₇ polyhedra.²⁴ Then one possibility of the shoulder at 3.81 Å is that of the second nearest Ti-O distance.

The titanium atoms are chelated by bzac in the solidified product as the authors' group clarified based on infrared absorption spectroscopy in previous papers.^{9,10} GPC measurements suggested that the solidified product prepared from the solution of Ti(OC₄H₉)₄ : bzac : H₂O : CH₃COCH₃ = 1 : 2 : 1 : 20 in mole ratios has two peaks in molecular weight distribution; one at *ca.* 22 000 and the other at *ca.* 8000.¹⁰ The molecular weights of 22 000 and 8000 correspond to polymerized species composed of *ca.* sixty and twenty TiO₆ octahedra, respectively, on the assumption that one bzac chelates one titanium atom. Then a structural model of the solidified product can be drawn as shown in Fig. 3, where several tens TiO₆ octahedra chemically modified with bzac are linked by corner- and edge-sharing.

Fig. 4a and b show the TMA and DSC curves, respectively, of the solidified product. Both curves clearly show a deflection around 10–30 °C, which is attributed to glass transition. Then the amorphous materials that are composed of bzac-modified TiO₆ octahedra linked by corner- and edge-sharing are now demonstrated to be a new class of glass materials.

Several studies have been conducted on glasses prepared by quenching the molten lead acetate.^{29–33} Venkatasubbaiah *et al.*³¹ and Murali *et al.*³² studied the local structure of lead acetate glasses using probe ions, reporting that the probe ions are present as octahedra. Ingram *et al.*³⁰ and Murali *et al.*³²

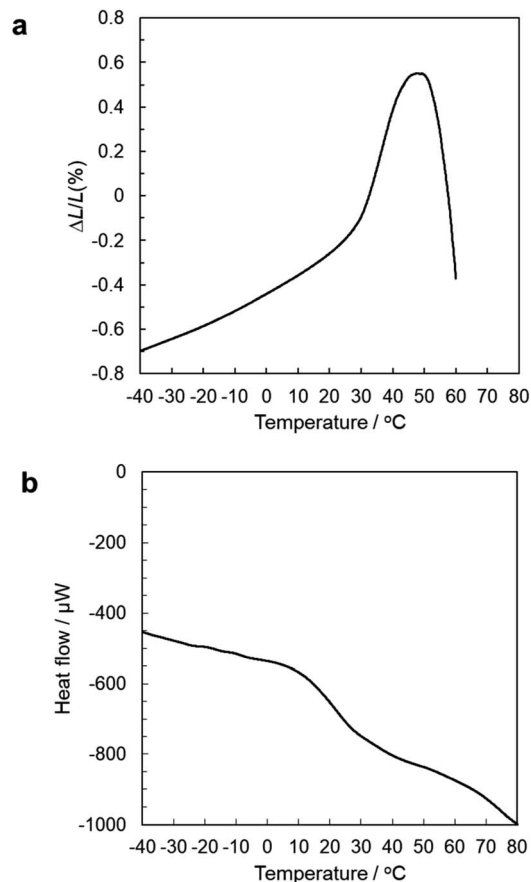


Fig. 4 (a) TMA and (b) DSC curves of the solidified product dried at 120 °C.

classified ordinary oxide glasses as polymeric glasses and nitrate and sulfate glasses as ionic glasses, recognizing that such lead acetate glasses as an intermediate between polymeric and ionic glasses. Acetate glasses obtained *via* thermal decomposition of magnesium acetate tetrahydrate are also reported, where glass transition was detected.^{34,35} Although no information is given on the linkages of the polyhedra in such acetate glasses, there is a possibility that they are composed of metal-oxo oligomers chemically modified by acetate ions. It should be noted, however, that the present route based on the hydrolysis of metal alkoxides in the presence of chelating agents may enlarge the possibilities to widen the compositions of such a class of glasses because of the flexible choices of metal elements and chelating agents.

Conclusion

The transparent materials obtained from titanium-*n*-butoxide solutions containing benzoylacetone were shown to be composed of TiO₆ octahedra linked by corner- and edge-sharing. The materials were also demonstrated to exhibit glass transition near at room temperature. The presented route provides optically transparent glassy materials of metal-oxygen polyhedra-based unique functions, for instance, high refractive



index, that can be shaped near at room temperature by extrusion or melt-casting.

Conflicts of interest

There are no conflicts to declare.

Acknowledgements

This work was supported by JSPS KAKENHI grant number JP18H02063. The HEXRD experiments were performed at the BL04B2 in SPring-8 with the approval of the Japan Synchrotron Radiation Research Institute (JASRI). The authors thank Prof. Miyuki Harada and Mr Yusuke Akazaki for the low temperature DSC measurements. The authors also thank Prof. Masahide Takahashi, Dr Yasuaki Tokudome and Mr Takuya Furukane for the preliminary experiments on the low temperature TMA measurements.

Notes and references

- 1 L. Rozes and C. Sanchez, *Chem. Soc. Rev.*, 2011, **40**, 1006–1030.
- 2 C. Sanchez, G. J. de A. A. Soler-Illia, F. Ribot, T. Lalot, C. R. Mayer and V. Cabuil, *Chem. Mater.*, 2001, **13**, 3064–3083.
- 3 P. Gouzerh and A. Proust, *Chem. Rev.*, 1998, **98**, 77–112.
- 4 D. L. Long, R. Tsunashima and L. Cronin, *Angew. Chem., Int. Ed.*, 2010, **49**, 1736–1758.
- 5 A. Proust, R. Thouvenot and P. Gouzerh, *Chem. Comm.*, 2008, 1837–1852.
- 6 U. Kortz, A. Muller, J. van Slageren, J. Schnack, N. S. Dalal, M. Dressel and M. Polyoxometalates, *Coord. Chem. Rev.*, 2009, **253**, 2315–2327.
- 7 J. B. Strong, G. P. A. Yap, R. Ostrander, L. M. Liable-Sands, A. L. Rheingold, R. Thouvenot, P. Gouzerh and E. A. Maatta, *J. Am. Chem. Soc.*, 2000, **122**, 639–649.
- 8 S. Oda, H. Uchiyama and H. Kozuka, *Chem. Lett.*, 2012, **41**, 319–321.
- 9 S. Oda, H. Uchiyama and H. Kozuka, *J. Sol-Gel Sci. Technol.*, 2014, **70**, 441–450.
- 10 S. Oda, H. Kozuka and H. Uchiyama, *J. Appl. Polym. Sci.*, 2015, **132**, 42653.
- 11 U. Schubert, *J. Mater. Chem.*, 2005, **15**, 3701–3715.
- 12 D. Hoebbel, T. Reinert and H. Schmidt, *J. Sol-Gel Sci. Technol.*, 1997, **10**, 115–126.
- 13 N. P. Bansal and R. H. Doremus, *Handbook of Glass Properties*, Academic Press, New York, 2013.
- 14 *Chalcogenide Glasses*, ed. J.-L. Adam and X. Zhang, Woodhead Publishing, Sawton, 2013.
- 15 *Halide Glasses for Infrared Fiberoptics*, ed. R. M. Almeida, Springer, Dordrecht, 1987.
- 16 C. Suryanarayana and A. Inoue, *Bulk Metallic Glasses*, CRC Press, Boca Raton, 2017.
- 17 *Polymer Glasses*, ed. C. B. Roth, CRC Press, Boca Raton, 2016.
- 18 U. P. Preiss and M. I. Saleh, *J. Pharm. Sci.*, 2013, **102**, 1970–1980.
- 19 T. Besara, P. Jain, N. S. Dalal, P. L. Kuhns, A. P. Reyes, H. W. Kroto and A. K. Cheetham, *Proc. Natl. Acad. Sci. U.S.A.*, 2011, **108**, 6828–6832.
- 20 T. D. Bennett, Y. Yue, P. Li, A. Qiao, H. Tao, N. G. Greaves, T. Richards, G. I. Lampronti, S. A. T. Redfern, F. Blanc, O. K. Farha, J. T. Hupp, A. K. Cheetham and D. A. Keen, *J. Am. Chem. Soc.*, 2016, **138**, 3484–3492.
- 21 S. Kohara, M. Itou, K. Suzuya, Y. Inamura, Y. Sakurai, Y. Ohishi and M. Takata, *J. Phys.: Condens. Matter*, 2007, **19**, 506101.
- 22 J. Demaison, H. D. Rudolph and A. G. Császár, *Mol. Phys.*, 2013, **111**, 1539–1562.
- 23 B. Prasai, B. Cai, M. K. Underwood, J. P. Lewis and D. A. Drabold, *Mater. Sci.*, 2012, **47**, 7515–7521.
- 24 K. Kaur, S. Prakash and N. Goyal, *J. Mater. Res.*, 2011, **26**, 2604–2611.
- 25 L. Cormier, P. H. Gaskell, G. Calas and A. K. Soper, *Phys. Rev. B*, 1998, **58**, 11322–11330.
- 26 F. Farges, G. E. Brown, A. Navrotsky, H. Gan and J. J. Rehr, *Geochim. Cosmochim. Acta*, 1996, **60**, 3039–3053.
- 27 K. Momma and F. Izumi, *J. Appl. Crystallogr.*, 2008, **41**, 653–658.
- 28 E. Dubler, R. Buschmann and H. W. Schmalte, *J. Inorg. Biochem.*, 2003, **95**, 97–104.
- 29 R. F. Bartholomew and S. S. Lewek, *J. Am. Ceram. Soc.*, 1970, **53**, 445–447.
- 30 M. D. Ingram, G. G. Lewis and J. A. Duffy, *J. Phys. Chem.*, 1972, **76**, 1035–1040.
- 31 A. Venkatasubbaiah, J. L. Rao and S. V. J. Lashman, *Polyhedron*, 1993, **12**, 1539–1543.
- 32 A. Murali, J. L. Rao, G. L. Narendra and T. Harinathudu, *Opt. Mater.*, 1997, **7**, 41–46.
- 33 M. A. Beltrão, M. L. Santos, M. E. Mesquita, L. S. Barreto, N. B. da Gosta Jr, R. O. Freire and M. A. Couto dos Santos, *J. Lumin.*, 2006, **116**, 132–138.
- 34 N. Onodera, H. Suga and S. Seki, *Bull. Chem. Soc. Jpn.*, 1968, **41**, 2222.
- 35 N. Koga, Y. Suzuki and T. Tatsuoka, *J. Phys. Chem. B*, 2012, **116**, 14477–14486.

